Supplementary Information

Mussel-inspired surface functionalization of porous carbon nanosheets using polydopamine and Fe^{3+}/tannic acid layers for high-performance electrochemical capacitors

Yeong A Lee,‡[ab] Jiyoung Lee,‡[c] Dae Wook Kim,[b] Chung-Yul Yoo,[a] Sang Hyun Park,[a] Jung Joon Yoo,[a] Seungchul Kim,[d] Bongsoo Kim,[c] Woo Kyung Cho,*[b] and Hana Yoon*[a]*

[a]*Korea Institute of Energy Research (KIER), Daejeon 34129, Republic of Korea.*

(e-mail: hanayoon@kier.re.kr)

[b]*Department of Chemistry, Chungnam National University, Daejeon 34134, Republic of Korea.*

(e-mail: wkcho@cnu.ac.kr)

[c]*Department of Chemistry, Korea Advanced Institute of Science and Technology (KAIST), Daejeon 34141, Republic of Korea.*

(e-mail: bongsoo@kaist.ac.kr)

[d]*Department of Optics and Mechatronics Engineering, College of Nanoscience and Nanotechnology, Pusan National University, Busan 46241, Republic of Korea.*

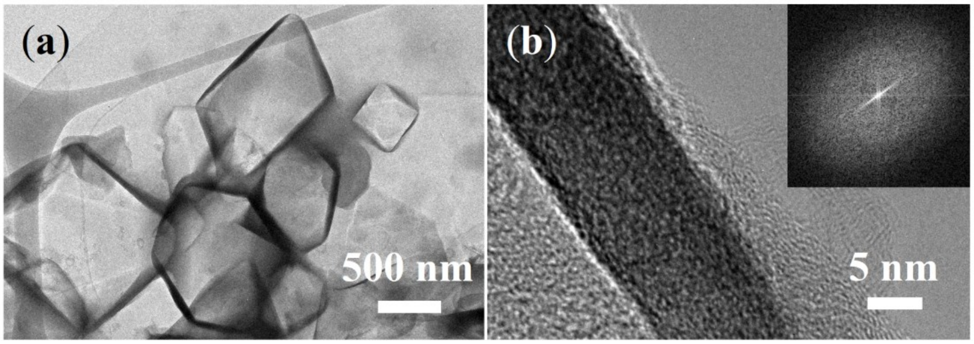

Fig. S1. (a) TEM image and (b) HRTEM image of IPCN850. The inset in (b) displays the FFT pattern of IPCN850, demonstrating their amorphous characteristic.

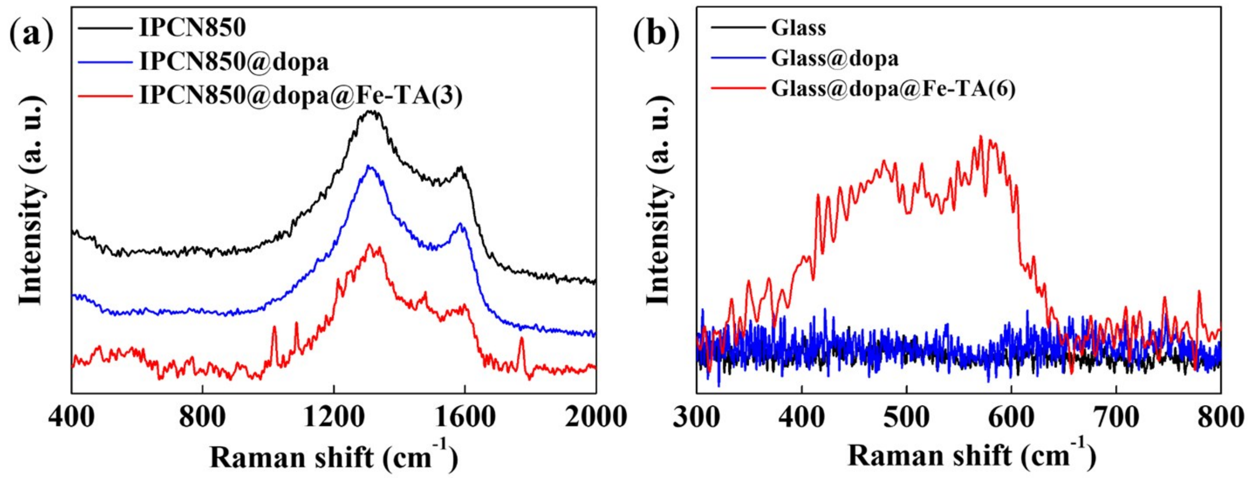

Fig. S2. The Raman spectra of (a) IPCN850, IPCN850@dopa, IPCN850@dopa@Fe-TA(3) electrodes and (b) bare glass, glass@dopa, glass@dopa@Fe-TA(6) samples.

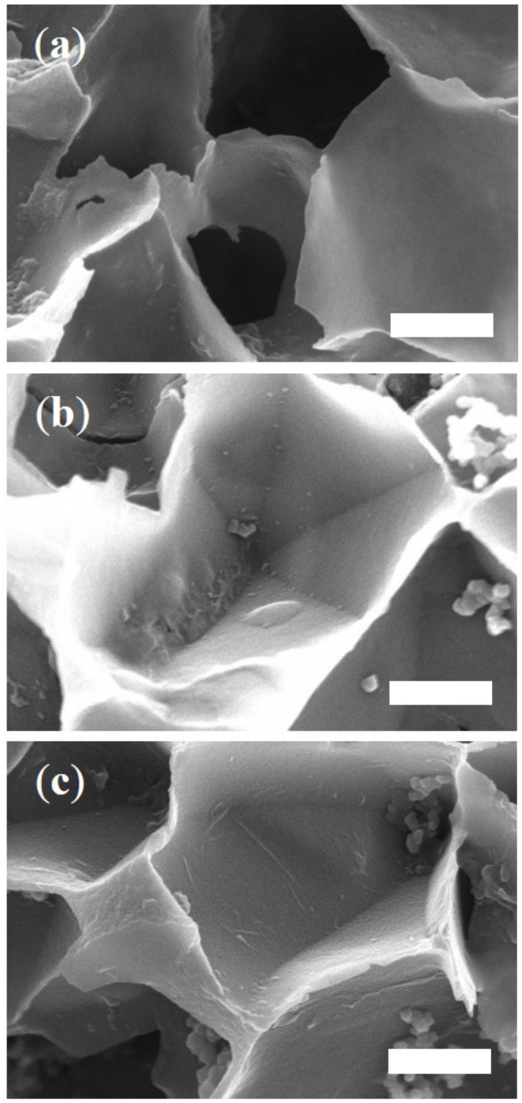

Fig. S3. FE-SEM images of (a) IPCN850 electrode, (b) IPCN850@dopa electrode, and (c) IPCN850@dopa@Fe-TA(3) electrode. (Scale bars represent 500 nm.)

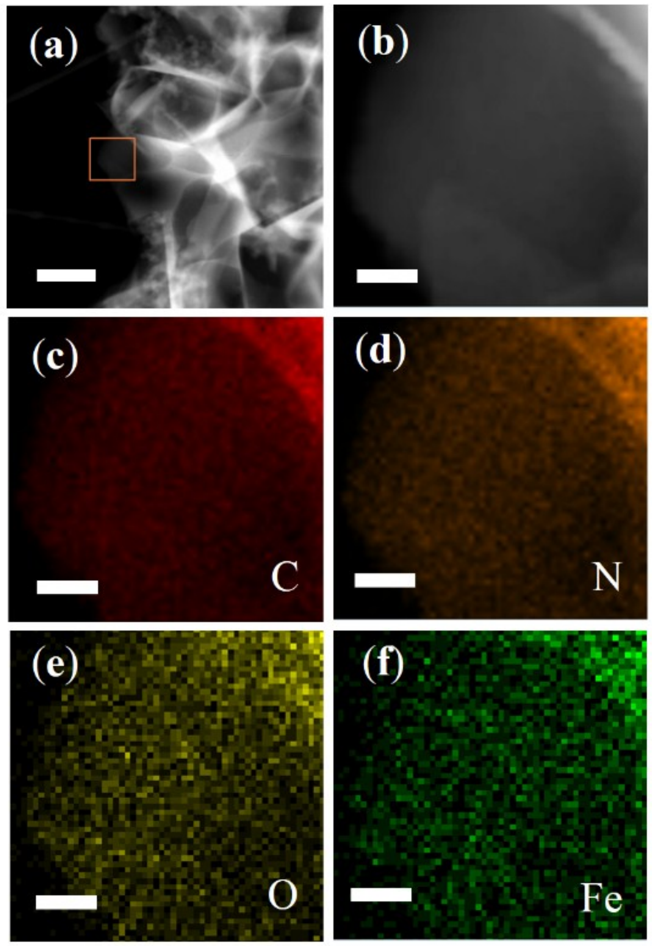

Fig. S4. (a,b) Dark-field TEM images of the IPCN850@dopa@Fe-TA(3). (c-f) TEM-EDX mapping of the IPCN850@dopa@Fe-TA(3). The C, N, O, Fe atoms are homogeneously distributed over the nanosheets. The scale bars represent 100 nm for the panel (a) and 20 nm for the panels (b-f).

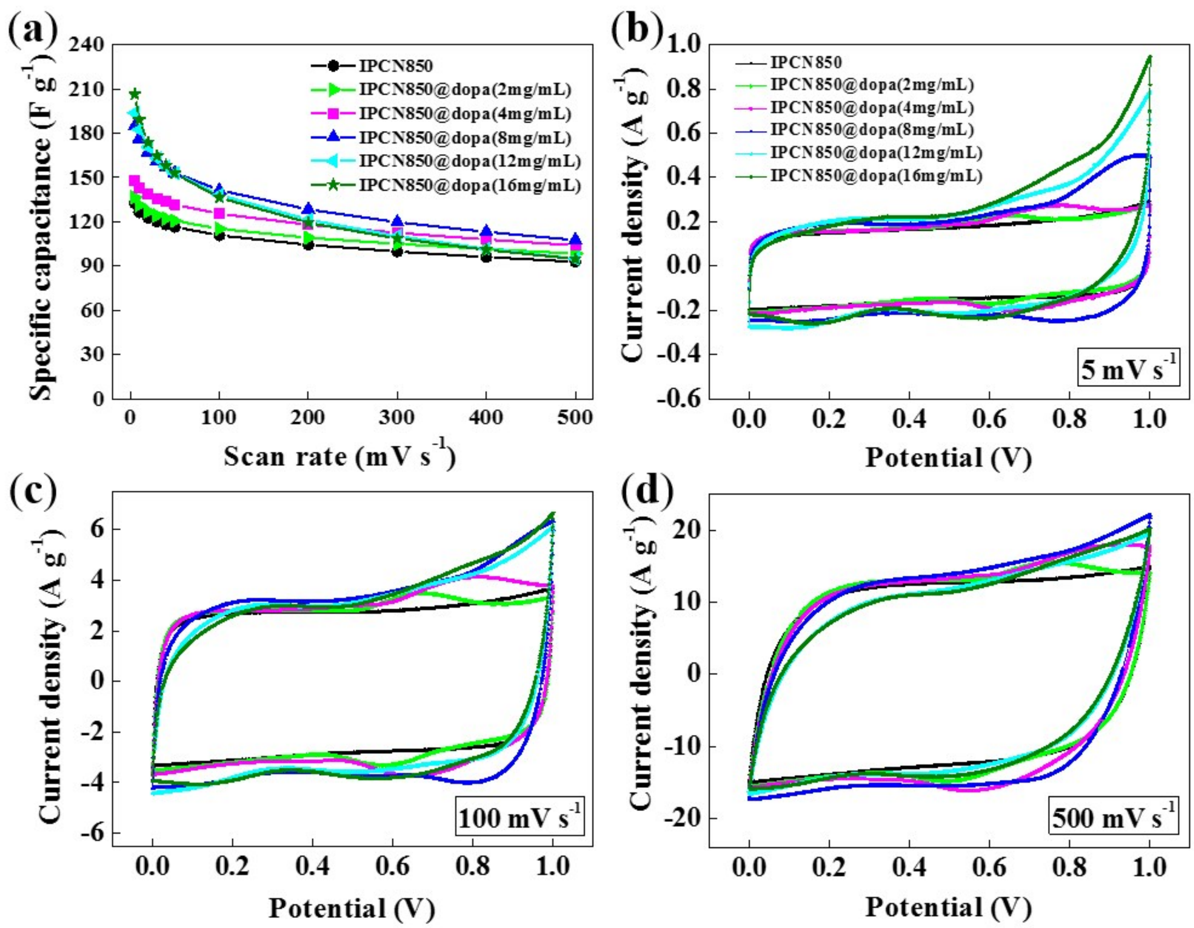

Fig. S5. (a) The specific gravimetric capacitances at different scan rates (5-500 mV s^{-1}) of IPCN850 and the polydopamine-coated IPCN850 (IPCN850@dopa) electrodes prepared with different concentrations (2, 4, 8, 12, or 16 mg mL^{-1}) of dopamine solution. CVs of IPCN850 and IPCN850@dopa electrodes with respect to the various concentrations of dopamine solution at the scan rate of (b) 5 mV s^{-1}, (c) 100 mV s^{-1}, and (d) 500 mV s^{-1}.

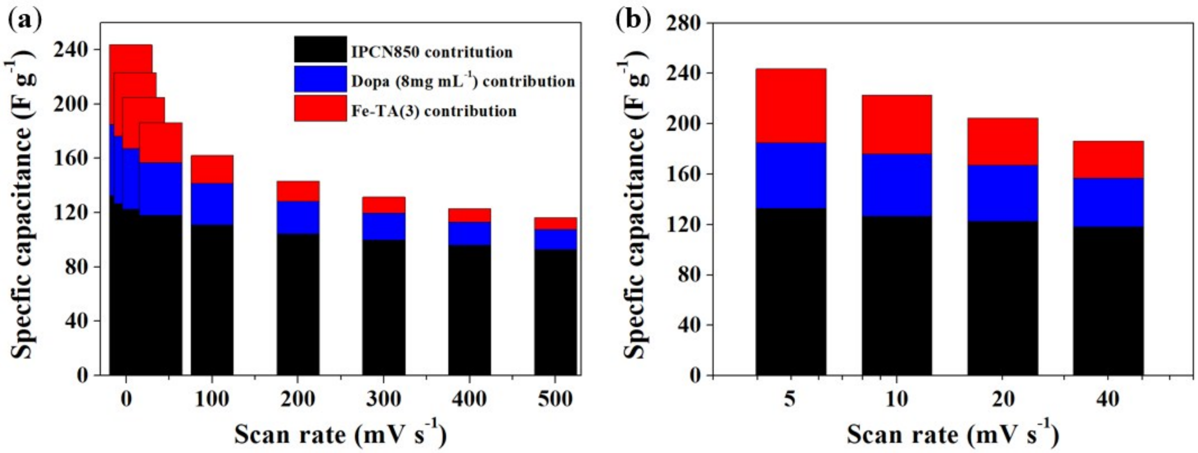

Fig. S6. Each contribution of IPCN850, polydopamine, and Fe^{3+}-tannic acid layers for IPCN850@dopa@Fe-TA(3) electrode to specific gravimetric capacitance at (a) different scan rates (5–500 mV s^{-1}) and (b) relatively low scan rates of 5–40 mV s^{-1}.

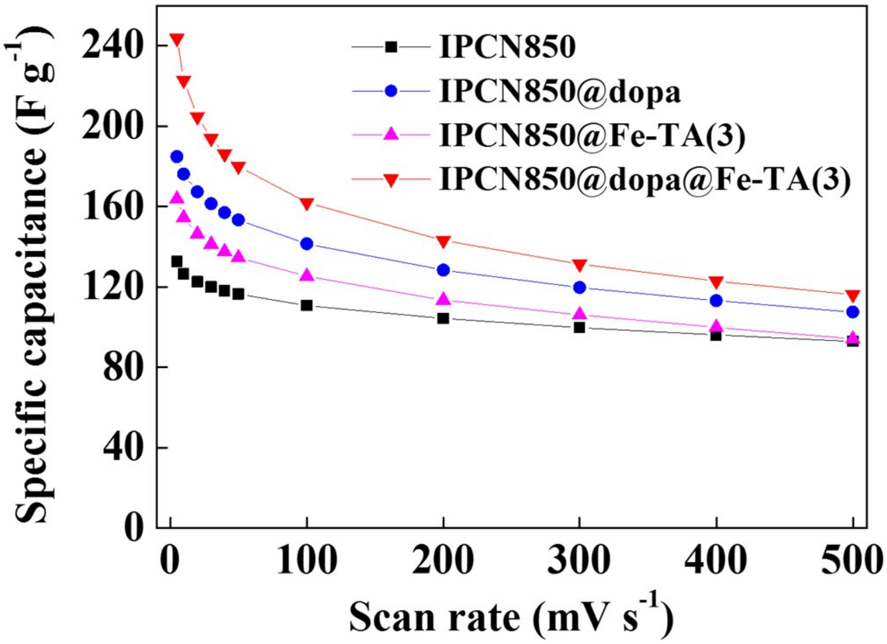

Fig. S7. Specific capacitances of IPCN850, IPCN850@dopa, IPCN@Fe-TA(3), and IPCN850@dopa@Fe-TA(3) electrodes at different scan rates (5-500 mV s^{-1}).

Table S1. EIS fitting parameters for IPCN850, IPCN@dopa, and IPCN850@dopa@Fe-TA(3) electrodes.

	IPCN850	IPCN850@dopa	IPCN850@dopa @Fe-TA(3)
R1 (Ω)	4.08×10^{-1} ($\pm 1.54 \times 10^{-2}$)	5.81×10^{-1} ($\pm 1.25 \times 10^{-2}$)	9.87×10^{-1} ($\pm 1.11 \times 10^{-2}$)
R2 (Ω)	2.51×10^{-1} ($\pm 1.91 \times 10^{-2}$)	1.06×10^{-1} ($\pm 1.58 \times 10^{-2}$)	2.52×10^{-1} ($\pm 1.64 \times 10^{-2}$)
Q1 ($\Omega^{-1} \cdot s^{-n}$)	2.30×10^{-4} ($\pm 1.17 \times 10^{-4}$)	2.31×10^{-5} ($\pm 3.09 \times 10^{-5}$)	7.55×10^{-5} ($\pm 4.08 \times 10^{-5}$)
n1	0.796 (±0.051)	1.053 (±0.123)	0.906 (±0.051)
WO-R (Ω)	1.57×10^{-1} ($\pm 2.50 \times 10^{-2}$)	3.56×10^{-1} ($\pm 3.73 \times 10^{-2}$)	2.78×10^{-1} ($\pm 3.13 \times 10^{-2}$)
WO-T (s)	1.34×10^{-2} ($\pm 2.43 \times 10^{-3}$)	2.55×10^{-2} ($\pm 3.36 \times 10^{-3}$)	7.30×10^{-3} ($\pm 9.92 \times 10^{-4}$)
WO-P	0.454 (±0.002)	0.432 (±0.003)	0.424 (±0.001)

Table S2. Morphology and electrochemical properties of the carbon-based electrodes and the electrodes functionalized with bio-inspired redox materials in aqueous electrolytes.

Ref.	Sample	Morphology	Electrochemical properties	
		Structure of active material	Specific capacitance of optimum electrodes	Capacitance retention (cycle)
This work	**IPCN@dopa@Fe-TA(3)**	**Nanosheet**	**244 F g^{-1} at 5 mV s^{-1} (1 M H_2SO_4)**	**92% (1000)**
Ref. [60]	Poly(norepinephrine)-functionlized graphene oxide sponge	Nanosheet	160 F g^{-1} at 10 mV s^{-1} (1 M H_2SO_4)	80% (2000)
Ref. [61]	Partially reduced graphene oxide/lignin/PEDOT composite	Irregular particle	144 F g^{-1} at 0.1 A g^{-1} (0.1 M $HClO_4$)	79% (1000)
Ref. [62]	PEDOT/lignin composite	Irregular particle	170 F g^{-1} at 1 A g^{-1} (0.1 M $HClO_4$)	83% (1000)
Ref. [63]	Surface-functionalized carbon nanotubes with kraft lignin	Nanotube	188 F g^{-1} at 0.1 A g^{-1} (0.5 M H_2SO_4)	93% (500)
Ref. [S1]	Dopamine-polypyrrole nanostructure	Nanofiber	273 F g^{-1} at 10 mV s^{-1} (2 M KCl)	-
Ref. [S2]	Catechol derivative-functionalized graphene aerogel	Nanosheet	188 F g^{-1} at 1 A g^{-1} (0.1 M $HClO_4$)	96% (10000)
Ref. [S3]	Polydopamine-functionalized graphene oxide/PEDOT	Irregular film	126 F g^{-1} at 1 A g^{-1} (0.1 M $LiClO_4$)	75% (300)
Ref. [S4]	Graphene-lignin composite	Nanosheet	211 F g^{-1} at 1 A g^{-1} (0.1 M $HClO_4$)	88% (15000)
Ref. [64]	Porous carbon derived from calcium citrate	Irregular particle	172 F g^{-1} at 1 mA cm^{-2} (6 M KOH)	95% (1000)
Ref. [65]	MOF-derived porous carbon	Rod or block shaped particle	159 F g^{-1} at 1 A g^{-1}	91% (200)

			(1 M H_2SO_4)	
Ref. [66]	Carbide-derived carbon aerogel	Irregular particle	137 F g^{-1} at 5 mV s^{-1} (1 M H_2SO_4)	-
Ref. [S5]	MOF-derived porous carbon	Nanosheet	119 F g^{-1} at 0.25 A g^{-1} (6 M KOH)	-
Ref. [67]	Activated carbon nanofiber	Fiber	105 F g^{-1} at 5 mV s^{-1} (6 M KOH)	103% (4000)

Table S3. Comparison of the specific capacities of the IPCN850, IPCN850@dopa, and IPCN850@dopa@Fe-TA(3) electrodes with other electrode materials.

To investigate the specific capacity of the electrode, we calculated the specific capacity according to the following equation [S6]:

$$W\ (mAh\ g^{-1}) = \frac{C_g \times \Delta V\ \times 1000\ (mAh\ g^{-1})}{3600}$$

where W is the specific capacity (mAh g^{-1}), C_g is the gravimetric specific capacitance and ΔV is the potential range of discharge.

Ref.	Sample	Specific capacity
This work	**IPCN850**	**36.8 mAh g^{-1} at 5 mV s^{-1} (1 M H_2SO_4) (calculated)**
	IPCN850@dopa	**51.3 mAh g^{-1} at 5 mV s^{-1} (1 M H_2SO_4) (calculated)**
	IPCN850@dopa@Fe-TA(3)	**67.7 mAh g^{-1} at 5 mV s^{-1} (calculated)**
Ref. [62]	PEDOT/lignin composite	34.1 mAh g^{-1} at 1 A g^{-1} (0.1 M $HClO_4$)
Ref. [72]	Activated carbon derived from Rapeseed dregs	51.2 mAh g^{-1} at 0.2 A g^{-1} (1 M H_2SO_4)
Ref. [73]	Activated carbon/Bi_2O_3 nanocomposite	39.32 mAh g^{-1} at 1 mA (9.83 mAh g^{-1} per cell) (30 wt% KOH)
Ref. [74]	$V_2O_5 \cdot 0.6H_2O$ nanoribbon	50.2 mAh g^{-1} at 2C (0.5 M K_2SO_4)
Ref. [S7]	Graphene/nickel-iron hexacyanoferrate nanocomposite	67.77 mAh g^{-1} at 0.5 A g^{-1} (0.5 M KNO_3)
Ref. [S8]	Graphite/polypyrrole composite	1.53 mAh g^{-1} at 1 mA cm^{-2} (0.3 M $NaClO_4$)

References

[S1] W. Zhang, Y. Zhou, K. Feng, J. Trinidad, A. Yu and B. Zhao, *Adv. Electron. Mater.*, 2015, **1**, 1500205.

[S2] J. Choi, M. -H. Yang and S. -K. Kim, *Appl. Surf. Sci.*, 2017, **422**. 316.

[S3] I. Cha, E. J. Lee, H. S. Park, J. -H. Kim, Y. H. Kim and C. Song, *Synth. Met.*, 2014, **195**, 162.

[S4] X. Geng, Y. Zhang, L. Jiao, L. Yang, J. Hamel, N. Giummarella, G. Henriksson, L. Zhang and H. Zhu, *ACS Sustainable Chem, Eng.*, 2017, **5**, 3553.

[S5] Y. Liu, J. Xu and S. Liu, *Micropor. Mesopor. Mat.*, 2016, **236**, 94.

[S6] H. Nishihara and T. Kyotani, *Adv. Mater.*, 2012, **24**, 4473.

[S7] S. Ghasemi, S. R. Hosseini and P. Asen, *Electrochim. Acta*, 2015, **160**, 337.

[S8] A. Faye, G. Dione, M. M. Dieng, J. J. Aaron, H. Cachet and C. Cachet, *J. Appl. Electrochem.*, 2010, **40**, 1925.